Functional single-cell analysis of T-cell activation by supported lipid bilayer-tethered ligands on arrays of nanowells

Alexis J. Torres[1], **Rita Lucia Contento**[1], **Susana Gordo**[3], **Kai W. Wucherpfennig**[3,4], and **J. Christopher Love**[1,2]

[1]Department of Chemical Engineering, Massachusetts Institute of Technology, Cambridge, MA 02139

[2]Koch Institute for Integrative Cancer Research, Massachusetts Institute of Technology, Cambridge, MA 02139

[3]Department of Cancer Immunology and AIDS, Dana-Farber Cancer Institute, Boston, MA 02115

[4]Program in Immunology, Harvard Medical School, Boston, MA 02115

Abstract

Supported lipid bilayers are an important biomolecular tool for characterizing immunological synapses. Immobilized bilayers presenting tethered ligands on planar substrates have yielded both spatio-temporal and structural insights into how T cell receptors (TCRs) reorganize during the initial formation of synapses upon recognition of peptide antigen bound to major histocompatibility complex (MHC) molecules. The prototypical configuration of these assays, however, limits the extent to which the kinetics and structure of the supramolecular activation clusters of the synapse (that occur in seconds or minutes) can be related to subsequent complex cellular responses, such as cytokine secretion and proliferation, occurring over hours to days. Here we describe a new method that allows correlative measures of both attributes with single-cell resolution by using immobilized lipid bilayers and tethered ligands on the surface of dense arrays of subnanoliter wells. This modification allows each nanowell to function as an artificial antigen-presenting cell (APC), and the synapses formed upon contact can be imaged by fluorescence microscopy. We show that the lipid bilayers remain stable and mobile on the surface of the PDMS, and that modifying the ligands tethered to the bilayer alters the structure of the resulting synapses in expected ways. Finally, we demonstrate that this approach allows the subsequent characterization of secreted cytokines from the activated human T cell clones by microengraving in both antigen- and pan-specific manners. This new technique should allow detailed investigations on how biophysical and structural aspects of the synapse influence the activation of individual T cells and their subsequent complex functional responses.

Introduction

T cells play a central role in regulating adaptive immune responses by interacting with other immune cells though direct receptor-mediated contact (as required for the induction of B cell differentiation) or by secreting cytokines and other mediators that regulate immune cell responses. Activation of T cells occurs when they engage cognate peptides bound to the major histocompatibility complex (MHC) molecules and other co-stimulatory molecules on the surface of an antigen-presenting cell (APC). This event initiates a signaling cascade that

*Correspondence should be addressed to: J. Christopher Love, Ph. D., Associate Professor in Chemical Engineering, Koch Institute for Integrative Cancer Research, Massachusetts Institute of Technology, 77 Massachusetts Ave., Bldg. 76-253, Cambridge, MA 02139-4307, Ph 617-444-9923, Fax 617-258-5042, clove@mit.edu.

leads to cytoskeletal rearrangement of actin, cell polarization, *de novo* protein synthesis and cytokine secretion, among other responses[1-3].

The structural interface between an APC and T cell, defined as the immunological synapse (IS), often comprises a distinct 'bull's eye' pattern of T cell receptor (TCR) surrounded by concentric lymphocyte function-associated antigen-1 (LFA-1)[4] (Fig. 1A), though other multifocal structures have also been observed[5, 6]. Following antigen recognition, microclusters of activated TCRs form at the region of contact on the cellular membrane and move centripetally to form a central supramolecular activation cluster (cSMAC), from which integrins are excluded and left in a surrounding region forming the SMAC (pSMAC)[7]. The functional role of the immunological synapse has not yet been fully elucidated. Continuous microcluster formation, and not formation of a cSMAC, appears necessary for activation and sustained signaling[1, 8], suggesting that the synapse may have other roles in regulating TCR signaling, possibly by acting as a site of receptor internalization and signal down-regulation[8, 9]. Nevertheless, the formation of the synapse is an important element of the induction of stimulated T cell responses that may have relevant roles *in vivo*[10, 11].

Both APCs and artificial substrates that mimic the surface of APCs have been used to characterize the spatio-temporal dynamics of T cell receptor activation and signal transduction at the synapse[2]. In particular, the combination of total internal reflection (TIRF) microscopy with ligands immobilized on supported lipid bilayers (SLBs), has allowed visualization of signaling molecules on activated T cells and investigation of the mechanisms governing TCR triggering[2, 12-14]. Both photolithography and soft lithography have facilitated patterning either SLBs or topographical features on their underlying planar substrates of glass or poly(dimethylsiloxane) (PDMS) to constrain the regional lateral mobility of SLBs[15]. The incorporation of tethered ligands such as recombinant peptide-loaded MHC (pMHC) complexes and co-stimulatory molecules (e.g., ICAM-1) into patterned SLBs have made it possible to examine mechanistic and structural aspects of immune receptor activation[14, 16-19]. Elastomeric arrays of microwells functionalized with supported lipid bilayers have also provided a means to spatially confine cells and to modulate the cellular microenviroment to investigate aspects of cellular adhesion[20].

Despite the utility of SLBs and patterned substrates for studying the molecular dynamics of the formation of the immunological synapse, these approaches have been constrained predominantly to analyses of early signaling events such as protein phosphorylation and redistribution of signaling proteins. It has been challenging in these experimental platforms to relate structural perturbations and transient interactions (e.g. co-stimulatory molecules, affinities of TCRs) to more complex cellular responses, such as cytokine release or proliferation, that evolve over long timescales (hours to days), with single-cell resolution. Assays for long-term functional responses usually rely on live APCs[21], soluble ligands[22], plate-bound ligands[23] or antibody-coated beads[24] for stimulation of bulk populations. These approaches make it difficult to define the relationship between T cell function and synapse organization. For example, ligands supported on substrates coated with antibodies immobilized by physical adsorption or covalent interaction do not allow the formation of dynamic microclusters and the immunological synapse formed on fluid membranes[23].

Here we present a new soft lithographic method that combines both imaging of synapses formed on mobile membranes and the capture of cytokines released from individual activated T cells using a technique called microengraving[25] (Fig. 1B). The approach uses dense elastomeric arrays of subnanoliter wells (nanowells) as a support for lipid bilayers with tethered recombinant ligands (e.g., pMHC). These arrays allow both the physical isolation of individual cells and the parallel activation of thousands of single T cells in either

pan-specific or antigen-specific manners. Following incubation of cells on the modified nanowells, the array can also be used for microengraving to assess the secretory responses of the cells. Microengraving is a method for printing matched protein microarrays where each element corresponds to the secreted proteins captured from individual nanowells. We find that the bilayer remains both stable and mobile, permitting imaging of the structure of the synapses formed by fluorescence microscopy and sampling of the secreted cytokines following activation by microengraving. The measured functional responses induced by tethered ligands on SLBs are comparable to those induced by conventional means (e.g., beads supporting activating antibodies to CD3 and CD28). This novel process for integrated single-cell analysis should enable new studies to relate structural features of immunological synapses with the subsequent functional responses by activated T cells, with control of the number of activation ligands and co-stimulatory molecules as well as relative ratios and densities of molecules presented.

Methods

Materials

Antibodies used for T cell activation were anti-human CD3 (clone UCHT1) and anti-human CD28 (clone CD28.2). Antibodies used to capture secreted cytokines were anti-human IL-2 (clone 5355, R&D) and anti-human IFNγ (clone 1-D1K, Mabtech). Anti-human IFNγ (clone 7-B6-1, Mabtech) and polyclonal anti-human IL-2 (R&D) detection antibodies were fluorescently labeled with Alexa Fluor 488 (Invitrogen) and Alexa Fluor 598 (Invitrogen), respectively, following the manufacturer's instructions. Rabbit anti-mouse IgG (Fcγ specific) antibodies used to prepare biotinylated Fab' constructs were purchased from Jackson ImmunoResearch (West Grove, PA). For the preparation of biotinylated constructs, (Fab')$_2$ fragments were treated with an excess of 2-mercaptoethylamine•HCl (Pierce, Thermo Scientific) in phosphate-buffered saline containing EDTA (PBS-EDTA,100 mM NaHPO$_4$, 150 mM NaCl, 0.1 M EDTA, pH 7.2) following the manufacturer instructions. The fragments were purified by size exclusion chromatography and reacted with ChromaLink™ Biotin Maleimide Reagent (Solulink, San Diego, CA). The ChromaLink biotin was used to quantify the number of biotins per Fab' fragment by UV-Vis spectrometry. The lipids used to prepare supported bilayers were: 1,2-dioleoyl-sn-glycero-3-phosphocholine (DOPC), 1,2-dioleoyl-sn-glycero-3-phosphoethanolamine-N-(lissamine rhodamine B sulfonyl) (Liss Rhod PE), 1,2-dioleoyl-sn-glycero-3-phosphoethanolamine-N-(cap biotinyl) (Biotinyl Cap PE) and 1,2-dioleoyl-sn-glycero-3-[(N-(5-amino-1-carboxypentyl)iminodiacetic acid)succinyl] (nickel salt) (18:1 DGS-NTA(Ni)) and were all purchased from Avanti Polar Lipids Inc. (Alabaster, AL). Dynabeads® Human T-Activator CD3/CD28 magnetic beads were purchased from Invitrogen. Soluble mono-biotinylated HLA-DR0401, either loaded with CLIP control peptide or hemagglutinin peptide 306-318, and soluble mouse ICAM-1 with a His$_{12}$-tag at the C terminus were prepared as described previously [21].

Culture of Influenza-specific T cell clones

A human T cell clone (HA:D7) specific for the influenza hemagglutinin peptide HA$_{306-318}$ presented by HLA-DR4 (*DRA,DRB1**04:01) has been described and characterized previously [21]. HA:D7 T cells were cultured in RPMI media supplemented with 10%(v/v) FBS, 2 mM GlutaMAX-I, 10 mM Hepes (all Invitrogen), 1%(v/v) human serum (Valley Biochemical) and 5 U/mL rIL-2 (Roche) as described previously [26]. T cells were starved for IL-2 for 2-4h before the experiment.

Isolation of human peripheral blood mononuclear cells (PBMCs) and enrichment of naïve T cells

Sample collection was approved by the institutional review board at Brigham and Women's Hospital and the MIT Committee On Use of Humans as Experimental Subjects (COUHES). Venous blood was drawn from healthy donors into lithium heparin tubes (Kendal). PBMCs from blood samples were separated using density centrifugation on Ficoll-Paque PLUS (GE Healthcare) and frozen with controlled gradual temperature decrease at a concentration of $5\text{-}10 \times 10^6$ cells/mL in 10% (v/v) dimethylsulfoxide (Sigma-Aldrich) and 90% (v/v) fetal calf serum (Atlanta Biologicals). After thawing, PBMCs were resuspended at 10^6 cells/mL in RPMI 1640 medium (Cellgro, Mediatech), supplemented with 10% (v/v) FBS, 2 mM L-glutamine, 10 mM HEPES, 100 U/mL penicillin, 100 mg/mL streptomycin, 0.1 mM non-essential amino acids, and 1 mM sodium pyruvate. $CD4^+CD45RA^+CD45RO^-$ T cells were enriched using the EasySep® Human Naive CD4+ T Cell Enrichment kit (STEMCELL Technologies Inc, VA, Canada) following the manufacturer's instructions. Enriched T cells were cultured overnight in supplemented RPMI media before the experiment.

Fabrication of PDMS arrays of nanowells

The array of nanowells was manufactured by injecting polydimethylsiloxane (PDMS, Dow Corning) prepared at a 10:1 base/catalyst weight ratio into a custom-built mold encasing a micropatterned silicon master. Arrays of nanowells were cured at 70 °C for 4-16 h. Each array comprised 72×24 blocks, each containing a 7×7 ($50\,\mu m \times 50\,\mu m \times 50\,\mu m$) subarray of nanowells, with a center-to-center distance of $100\,\mu m$, or a 12×12 ($30\,\mu m \times 30\,\mu m \times 30\,\mu m$) with center to center distance of $60\,\mu m$. The PDMS arrays adhered directly to a $3'' \times 1''$ glass slide forming a 1 mm thick layer.

Preparation of supported lipid bilayers

Lipids were dissolved and mixed at different molar ratios in chloroform. The solution of lipids was dried under a stream of nitrogen, and the remaining solvent was removed by vacuum for 6 h or more. The lipid mixture was resuspended in Tris buffer (10 mM Tris, 150 mM NaCl, pH 7.6) at a final concentration of 1 mM and extruded >6 times with a 100 nm pore membrane before use.

The PDMS array of nanowells was plasma oxidized for 90-120 s using a Harrick Plasma cleaner (Model PDC-001,115V) and the liposomes were directly deposited to the surface and allowed to settle for 10-15 min. The surfaces were rinsed with deionized water to remove excess liposomes. Substrates were kept hydrated to prevent degradation of the lipid bilayer. The lipid bilayer was blocked with $100\,\mu g/mL$ BSA or 3% (w/v) casein in PBS for 45 min before use. For SLBs containing Biotin-Cap PE, the bilayer was incubated with 1 $\mu g/mL$ of streptavidin in a 0.25% (w/v) solution of human serum albumin (HSA) in PBS followed by incubation with the appropriate mono-biotinylated protein.

For activation using antibodies, streptavidin-containing SLBs were first incubated for 45 min with 1 $\mu g/mL$ of mono-biotinylated anti-mouse (Fcγ specific) Fab' in 0.25% (w/v) HSA/ PBS. The substrate was then incubated for at least 1 h with anti-human CD3, anti-human CD28, or anti-human CD3 and His-tagged ICAM-1 at 1$\mu g/mL$. For antigen-specific activation, the SLB was incubated with 1$\mu g/mL$ of mono-biotinylated peptide loaded MHC (pMHC) and His-tagged ICAM-1. His-tagged ICAM-1 was immobilized on bilayers containing 5 mol% DGS-NTA(Ni). The device was rinsed extensively with PBS before adding the cells.

Fluorescence Recovery After Photobleaching (FRAP)

For fluorescence recovery experiments, PDMS substrates were covered with a No. 2 Lifter slip and imaged using an Applied Precision DeltaVision system with a 60x/1.4NA objective. The instrument was equipped with an Olympus X71 microscope with XYZ nano-motion stage, halogen transmitted light source, a solid state illumination (SSI) module coupled to a fiber optic cable and a Photometrics CoolSNAP HQ camera. Photobleaching experiments were performed using the 568 nm laser line coupled to a fiber optic. Photobleaching experiments were performed both inside the nanowells and in planar regions outside the wells to probe for membrane fluidity. To avoid the introduction of artifacts from the optical variances at the edges of the nanowells, the diffusion coefficient and mobile fractions were estimated using data from planar regions outside of wells; qualitatively the responses inside wells were similar. A custom MATLAB routine was used to measure the 1/e gaussian profile for each bleach spot to account for sample variations in the bleach profile. After correcting for bleaching, the recovery curve was fitted to a simple 2D diffusion model that assumes a gaussian beam profile[27]. The diffusion coefficient (D) was estimated from: $D = w^2/(4t_{1/2})$ where w is the laser spot size radius at $1/e^2$ and $t_{1/2}$ is the recovery time constant.

Imaging the formation of immunological synapses inside nanowells

SLBs were generated by applying DOPC liposomes containing 5 mol% DGS-NTA(Ni) and 0.1 mol% biotin-Cap-PE lipids on the PDMS array of nanowells. Fluorescently-labeled Alexa Fluor 488-streptavidin was used to immobilize and visualize either anti-CD3 or pMHC, and Alexa Fluor 647-labeled ICAM-1 (His 12) was used to visualize the pSMAC. ICAM-1 bound to the lipid bilayer by means of multiple histidine interactions with NTA(Ni)-linked lipid head groups. HA:D7 T cells were deposited into the array in supplemented RPMI media (without IL-2) and incubated with the SLBs for 20-70min at 37°C during live-cell imaging. Wells of 30 μm depth were used instead of 50μm wells to accommodate the optimal working distance (depth) of the objective.

Preparation of antibody-coated capture slide for microengraving

Capture antibodies were diluted in borate buffer (50 mM sodium borate, 8 mM sucrose, and 50 mM NaCl, pH 9.0) to a final concentration of 10 μg/mL and deposited on the surface of poly-L-lysine coated slides (prepared as described previously[25]) for 1 h at room temperature. Slides were blocked with 3% non-fat milk in PBST (PBS with 0.05% (v/v) Tween 20) for 30 min at room temperature and washed with PBS before placing them into contact with the PDMS array of nanowells.

Microengraving

A suspension of T cells was dispensed onto the surface of the nanowells, modified with a supported lipid bilayer, in HL-1 media (supplemented with 2 mM L-glutamine, 10 mM HEPES, 100 U/mL penicillin, 100 mg/mL streptomycin, 0.1 mM non-essential amino acids, and 1 mM sodium pyruvate), and allowed to settle into the wells. In the case where cells were stimulated with anti-CD3/CD28 beads, the surface of the PDMS was pre-treated with an oxygen plasma for 2 min before adding cells and CD3/CD28 beads. For antigen-specific clones, HA:D7 T cells were cultured inside the wells in supplemented RPMI media (without IL-2). The concentration of suspended cells applied to the array was optimized empirically to maximize well occupancy with single cells (typically ~30% of wells).

After incubation of the cell-loaded wells, a glass slide coated with capture antibodies was then placed onto the loaded array for printing. The microarray and glass slide were held together by compression in a hybridization chamber (Agilent Technologies, G2534A) and

incubated for 1h at 37 °C with 5% CO_2. The glass slide was then separated from the array and placed in PBS.

Detection of captured cytokines

After microengraving, slides were incubated for 30 min with blocking buffer (PBS, 10mg/mL BSA, 0.05 % (v/v)Tween-20, 2% mouse serum and 2 mM sodium azide), washed with PBST(PBS+ 0.05% v/v Tween-20), and then incubated with fluorescent antibodies (Alexa Fluor 488 anti-IFNγ and Alexa Fluor 594 anti-IL-2) at 1 μg/mL for 45 min at 25°C. The slides were washed with PBST and PBS, rinsed briefly with water, and dried with a N_2 stream. Reference slides were generated at the end of each experiment with the same detection antibodies used on the printed slides. For reference slides, antibodies were diluted in water, spotted onto blank poly-L-lysine slides (1 μL/spot), and the reference slides were dried under vacuum. Slides were scanned using a Genepix 4200AL microarray scanner (Molecular Devices). The median fluorescence intensity of each spot was extracted using Genepix Pro.

On-chip image-based cytometry

Before imaging, T cells were stained with calcein violet (Invitrogen) and SYTOX green (Invitrogen). The cell-loaded arrays of nanowells were mounted face-up on the microscope with a coverslip placed on top of the array. Images were acquired on an automated inverted epifluorescence microscope (Carl Zeiss). Transmitted light and epifluoresence micrographs were collected block-by-block (7×7 microwells per block). The resulting collection of images was analyzed using a custom program to determine the number of cells present in each well and the mean fluorescent intensity of each label. Only viable T cells (calcein fluorescent intensity >3 standard deviations above background) were considered for the analysis.

Data analysis

Data extracted from both on-chip cytometry and printed cytokines were matched in Microsoft Excel using unique identifiers assigned to each well within the array. The dataset was filtered to include wells containing only single cells. To compensate from signal bleed-through and convert the measured fluorescence intensity for the captured cytokines from a given cell into a rate of secretion, the data from the standard calibration curve (from reference slides) prepared with known amounts of detection antibodies was used to convert measured intensities to a number of molecules, as described previously[25].

Results

Formation and stability of supported lipid bilayers on PDMS

The stability of supported lipid bilayers have been studied most extensively on a small number of oxidized surfaces, such as glass, silicon oxide and quartz and oxidized polydimethylsiloxane (PDMS)[20, 28-31]. Supported bilayers have also been used as a substrate for cell culture,[20, 32] but the stability, fluidity and compatibility of lipid bilayers supported on PDMS for long-term cell culture have not been well characterized. The surface of PDMS becomes highly hydrophilic upon plasma oxidization due to the formation of interfacial oxide groups,[33, 34] but this interface can change over time, restoring the native hydrophobicity[35]. This reversion could pose a problem for the stability of the SLB, which is sensitive to the chemistry of the support. To characterize the PDMS-supported lipid membrane, we performed a series of photobleaching recovery experiments to assess changes in the fluidity of the membrane over time. Supported lipid bilayers comprising 97 mol % DOPC, 2 mol% Biotin-Cap PE and 1 mol % Liss Rhod PE were formed on the surface of an

oxidized PDMS slab and kept at room temperature in a PBS solution with 100μg/mL BSA during the duration of the experiment. The rhodamine conjugated to the Liss Rhod PE lipids was photobleached for 0.3 s within a defined region of the SLB and the recovery of fluorescence intensity was subsequently monitored by microscopy (Fig. 2A,B). Fluorescence recovery was also measured after long incubations at 37°C (72 and 96 h) and no significant differences in the mobile fraction were observed compared to the values obtained at 25°C (data not shown). The full recovery of signal in the bleached region demonstrated that the bilayer remained highly mobile, even at physiological temperature.

From these experiments, we determined the diffusion coefficient and the mobile fraction for lipids in the SLB at different times after bilayer deposition (Fig. 2C). Over 96 h, the diffusion constants ranged from 1-1.5 μm^2/s and the mobile fraction of the lipids varied from 80-97%, consistent with previous reports[20]. Most studies using SLBs to investigate signaling via TCRs have employed glass substrates as supports, where diffusion coefficients are typically ~3 μm^2/s—2-3 times higher than those observed on the oxidized PDMS[20]. The slightly reduced diffusion coefficient for the lipids supported on the PDMS, or the overall stability of the bilayer on this substrate, could potentially hinder the redistribution of receptors presented on a cell's surface upon contact with tethered ligands. We found, however, that SLBs on PDMS were highly stable and mobile even under prototypical conditions for cell culture. The diffusion coefficient changed little over time and the reduced diffusion had no apparent effect on the formation of the immunological synapse (as described below).

Support and activation of primary T cells in supported lipid bilayer-coated nanowells

To evaluate the suitability of the bilayer-coated PDMS for characterizing primary human T cells, we first cultured T cells from peripheral blood in nanowells containing SLBs (99 mol % DOPC and 1mol% Liss Rhod PE) for 72 h at 37°C in HL-1 media, and then imaged them to determine their viability as well as the integrity of the supported bilayers in contact with cells (Fig. 2D). Cell viability was reduced by 30% after culture for 72 h, but was indistinguishable from that of cells cultured only on oxidized PDMS. (We note that, in the absence of stimulating factors to induce T cell activation, it is expected that a significant fraction of primary human T cells will die over days in culture, regardless of the substrate.) These data show that supported bilayers do not significantly degrade during *in vitro* culture of these non-adherent cells, and remain stable for at least 72 h in the presence of viable T cells.

Given the stability of the bilayers *in vitro*, we then tested the feasibility of using arrays of nanowells coated with SLBs to activate T cells and monitor their long-term functional responses, such as cytokine and chemokine secretion. Following antigen-independent stimulation for 5 h in arrays of nanowells containing either magnetic beads or PDMS-supported lipid bilayers coated with a combination of anti-CD3/CD28, the secretion of IL-2 and IFNγ was characterized by microengraving with single-cell resolution (Fig. 3). Both methods of presenting the activating antibodies were efficient at inducing cytokine secretion from naive T cells; in contrast, SLBs containing the non-activating anti-CD19 (as a control) did not induce any secretion (data not shown). In addition, we observed that the majority of cells remained viable (~97%) after 10 h of incubation on the arrays, suggesting that short-term cultures to assess secretory responses by primary T cells in SLB-modified PDMS nanowells are feasible.

The total percentage of secreting cells upon activation was below ~5%, whether stimulated with beads or SLBs. This observation is consistent with previous studies on secretion from T cells activated by soluble stimuli and measured by microengraving[3637]. The relative fraction of cells secreting IL-2, IFNγ or both was also similar between the two configurations used

here for stimulation (Fig. 3B). In addition to the comparable percentages of secreting cells observed, the quantitative rates of secretion for both cytokines measured were similar between the two approaches (Fig. 3C). Together, these measurements demonstrate that nanowells coated with SLBs bearing tethered activating ligands can induce functional responses, such as cytokine secretion, by primary human T cells and be detected by microengraving.

Characterization of immunological synapses and functional responses in nanowells

The fluidity and stability of the lipid bilayers on the PDMS suggested that it should be possible to visualize the structure of the immunological synapses formed on the basal surfaces of the nanowells, and monitor the subsequent functional responses. We tested this hypothesis using a human CD4+ T cell clone (HA:D7) that exhibits specificity for the influenza hemagglutinin peptide 306-318 ($HA_{306-318}$) presented by HLA-DR4 (*DRA, DRB1**04:01). Nanowells supporting bilayers presenting recombinant monomers of HLA-DR4 bearing the HA peptide and ICAM-1 induced clustering of TCRs on these cells with the formation of immunological synapses consistent with the typical bull's eye pattern comprising the cSMAC and pSMAC (Fig. 4A). This structure was similar to that formed with anti-CD3 and ICAM-1 as a positive control (Fig. 4B), though the antigen-induced cSMAC was typically smaller in size and less dense by comparison. When ICAM-1 was absent from the bilayer and the density of anti-CD3 increased (biotin-Cap PE lipids ~2 mol %), small, decentralized microclusters of TCR formed instead of the organized cSMAC (Fig. 4C). Together, these data show that nanowells modified with ligand-presenting SLBs can induce synapses in a manner similar to that on planar glass substrates.

We then incubated arrays of nanowells supporting lipid bilayers bearing both ICAM-1 and class II MHC monomers (HLA-DR4) for 2 h and measured the secretion of IL-2 and IFNγ for 2 h (4 h total stimulation) by microengraving. Arrays with monomers of MHC bearing $HA_{306-318}$ exhibited robust responses compared to a non-stimulating control with an irrelevant peptide (CLIP), demonstrating antigen-specific responses from the T cell clones (Fig. 5A). For this clone, we found that the secretion of IFNγ represented the majority of the responses (31%), with a small fraction of cells secreting IL-2 either in combination with IFNγ or alone (1%) (Fig. 5B). We note that the functional heterogeneity observed here is common for T cell clones, with only a fraction of the cells exhibiting cytokine production[25]. Consistent with our previous analyses of secreted cytokines from activated T cells, we also observed that the median rate of secretion for IFNγ was higher than that for IL-2 (Fig. 5C).

Discussion

We present here a new nanowell-based approach that takes advantage of microengraving to enable a quantitative, correlative analysis of the structure of the immunological synapses formed by T cells and the functional responses induced with single-cell resolution. This methodology relies on modified nanowells that support stable lipid bilayers with tethered ligands to act as mimics of APCs for stimulating individual isolated cells. In this work, we have demonstrated that not only we can stimulate cells in a way that allows formation of synapses that could be correlated to downstream cellular responses, but we can also quantify some of the responses (cytokine secretion) at the single-cell level to investigate heterogeneities in the functional responses within populations of cells. This flexible and tunable tool has potential to reconcile the relationships between structural (e.g. formation of the cSMAC and pSMAC vs. decentralized clusters) and biophysical (e.g. binding affinity, kinetics of TCR-pMHC and ligand density) aspects of the synapse with long-term cellular responses such as cytokine secretion and cell proliferation.

The use of supported lipid bilayers to present peptide-loaded MHC class II monomers and co-stimulatory molecules to T cells overcomes technical challenges with other methods for presenting antigen to T cells in nanowells. We have previously shown that absorption of recombinant peptide-loaded MHC class II monomers on the surface of PDMS, along with antibodies for co-stimulation, can trigger antigen-specific activation of human T cells[38]. This simple approach to modify the surfaces of nanowells by adsorption is sufficient for short-term measurements, but the interfaces formed by this method are poorly defined, with uncertain uniformity, and limited stability during long periods of culture (> 12 h). Beads coated with anti-CD3 and anti-CD28 antibodies are also often used to stimulate populations of cells in bulk for conventional assays measuring functional responses of T cells. We have used these particles as a control to activate cells in wells, but the distribution of particles into wells is not uniform, governed by Poisson statistics. This uneven application means that some cells do not receive stimulation in a given experiment, and thus, the efficiency of profiling functional responses is reduced. In contrast, the fluidity of the SLBs applied to the PDMS promotes uniform coverage of the nanowells, and thus, consistent exposure of all cells to specific stimuli is possible. (We do note that, although the ligand density in the lipid bilayer can be precisely defined, the exact local concentration of ligand within the IS cannot be controlled due to the mobility of the bilayer. Thus, more complex surface modifications, such those used previously to investigate clustering of receptors at the IS[18], could further improve investigations on the effects of local density of pMHC at the IS on the modulation of T cell responses.) Moreover, the lipid bilayers present a more inert and physiologically relevant substrate that can minimize non-specific binding and unwanted artifacts[39].

Another advantage of using SLBs to present stimulating ligands to cells in nanowells is the potential to test defined combinations of activating ligands and co-stimulatory molecules systematically[40]. Many adhesion, co-stimulatory and co-inhibitory molecules contribute to the outcome of T cell activation, which can be tested in combination with defined peptide-MHC complexes. The flexibility of the chemistries for tethering ligands to the bilayers makes it feasible to examine how co-stimulatory and co-inhibitory molecules influence the synaptic structure and functional responses for a range of antigen-specific T cells with different pMHC specificities. The ability to prepare well-defined interfaces for antigen-specific activation in this manner also provides a means to standardize antigen presentation for high-throughput, single-cell analysis of populations of T cells for antigen specificity [41][42].

Using SLB-tethered ligands to activate individual T cells inside wells in combination with microengraving has potential to address many open questions that remain regarding the relationship between TCR ligand potency (characterized by the binding affinity and kinetics) and pMHC densities in regulating TCR-mediated T cell activation. We have recently shown that self-reactive T cells form unusual synapses and can retain a high degree of motility on SLB displaying peptide-MHC and ICAM-1. A major advantage of this technique is that highly motile cells are confined in individual wells and can thereby be tracked over extended periods of time. The system may also enable *ex vivo* analysis of synapse formation by primary T cells that recognize defined peptide-MHC complexes. Such studies could assess the relationship between synapse formation and *ex vivo* function of T cells isolated from tissues, such as pancreatic β cells from mice with type 1 diabetes or tumor-infiltrating T cells. Previous studies have provided evidence that high affinity ligands behave as strong agonists and that increasing the density of low affinity pMHCs can compensate for the potency of the TCR-pMHC interaction[43]. All these studies have depended on the use of APCs to present the pMHC to measure long-term cellular responses, which introduces more experimental variables due to the heterogeneous complexities of these cell-cell interactions. In addition, measurements in these assays yield only ensemble averages that cannot resolve how the responses are distributed among the population of cells (e.g., uniform distributions

or bimodal behaviors). For example, here we have shown that even within a clonal population of T cells, the patterns of secretions are not uniform and only a small fraction of cells secrete cytokines at a given time after stimulation. The approach introduced here should overcome the limitations of existing approaches by allowing specific control in the type of pMHC ligands, co-stimulatory molecules and the density of ligands presented on a fluid lipid bilayer. Uncovering the structure-function relationships between the molecular aspects of antigen presentation and T cell responses should improve our knowledge in T-cell-mediated diseases such as multiple sclerosis and type 1 diabetes.

Acknowledgments

References

1. Campi G, Varma R, Dustin ML. The Journal of Experimental Medicine. 2005; 202:1031–1036. [PubMed: 16216891]

2. Huppa JB, Davis MM. Nat Rev Immunol. 2003; 3:973–983. [PubMed: 14647479]

3. Dustin ML, Cooper JA. Nat Immunol. 2000; 1:23–29. [PubMed: 10881170]

4. Dustin ML, Chakraborty AK, Shaw AS. Cold Spring Harbor Perspectives in Biology. 2010; 2:1–14.

5. Brossard C, Feuillet V, Schmitt A, Randriamampita C, Romao M, Raposo G, Trautmann A. European Journal of Immunology. 2005; 35:1741–1753. [PubMed: 15909310]

6. Tseng S-Y, Waite JC, Liu M, Vardhana S, Dustin ML. The Journal of Immunology. 2008; 181:4852–4863. [PubMed: 18802089]

7. Grakoui A, Bromley SK, Sumen C, Davis MM, Shaw AS, Allen PM, Dustin ML. Science. 1999; 285:221–227. [PubMed: 10398592]

8. Yokosuka T, Sakata-Sogawa K, Kobayashi W, Hiroshima M, Hashimoto-Tane A, Tokunaga M, Dustin ML, Saito T. Nat Immunol. 2005; 6:1253–1262. [PubMed: 16273097]

9. Varma R, Campi G, Yokosuka T, Saito T, Dustin ML. Immunity. 2006; 25:117–127. [PubMed: 16860761]

10. Friedman RS, Beemiller P, Sorensen CM, Jacobelli J, Krummel MF. The Journal of Experimental Medicine. 2010; 207:2733–2749. [PubMed: 21041455]

11. Azar GA, Lemaître F, Robey EA, Bousso P. Proceedings of the National Academy of Sciences. 2010; 107:3675–3680.

12. Cebecauer M, Spitaler M, Sergé A, Magee AI. Journal of Cell Science. 2010; 123:309–320. [PubMed: 20130139]

13. Fooksman DR, Vardhana S, Vasiliver-Shamis G, Liese J, Blair DA, Waite J, Sacristán C, Victora GD, Zanin-Zhorov A, Dustin ML. Annual Review of Immunology. 2010; 28:79–105.

14. Mossman KD, Campi G, Groves JT, Dustin ML. Science. 2005; 310:1191–1193. [PubMed: 16293763]

15. Yu, C-h; Groves, J. Medical and Biological Engineering and Computing. 2010; 48:955–963. [PubMed: 20559751]

16. Torres AJ, Wu M, Holowka D, Baird B. Annual Review of Biophysics. 2008; 37:265–288.

17. Torres AJ, Vasudevan L, Holowka D, Baird BA. Proceedings of the National Academy of Sciences. 2008; 105:17238–17244.

18. Manz BN, Jackson BL, Petit RS, Dustin ML, Groves J. Proceedings of the National Academy of Sciences. 2011

19. Dustin ML, Groves JT. Annual Review of Biophysics. 2012; 41:543–556.

20. Andreasson-Ochsner M, Romano G, Hakanson M, Smith ML, Leckband DE, Textor M, Reimhult E. Lab on a Chip. 2011; 11:2876–2883. [PubMed: 21773619]

21. Schubert DA, Gordo S, Sabatino JJ, Vardhana S, Gagnon E, Sethi DK, Seth NP, Choudhuri K, Reijonen H, Nepom GT, Evavold BD, Dustin ML, Wucherpfennig KW. The Journal of Experimental Medicine. 2012; 209:335–352. [PubMed: 22312112]

22. Bekoff M, Kubo R, Grey H. The Journal of Immunology. 1986; 137:1411–1419. [PubMed: 3489033]

23. Bunnell SC, Hong DI, Kardon JR, Yamazaki T, McGlade CJ, Barr VA, Samelson LE. The Journal of Cell Biology. 2002; 158:1263–1275. [PubMed: 12356870]

24. Bonyhadi M, Frohlich M, Rasmussen A, Ferrand C, Grosmaire L, Robinet E, Leis J, Maziarz RT, Tiberghien P, Berenson RJ. The Journal of Immunology. 2005; 174:2366–2375. [PubMed: 15699173]

25. Han Q, Bradshaw EM, Nilsson B, Hafler DA, Love JC. Lab on a Chip. 2010; 10:1391–1400. [PubMed: 20376398]

26. Wucherpfennig KW, Sette A, Southwood S, Oseroff C, Matsui M, Strominger JL, Hafler DA. The Journal of Experimental Medicine. 1994; 179:279–290. [PubMed: 7505801]

27. Axelrod D, Koppel DE, Schlessinger J, Elson E, Webb WW. Biophysical journal. 1976; 16:1055–1069. [PubMed: 786399]

28. Hovis JS, Boxer SG. Langmuir. 2001; 17:3400–3405.

29. Lenz P, Ajo-Franklin CM, Boxer SG. Langmuir. 2004; 20:11092–11099. [PubMed: 15568862]

30. Nye JA, Groves JT. Langmuir. 2008; 24:4145–4149. [PubMed: 18303929]

31. Cremer PS, Boxer SG. The Journal of Physical Chemistry B. 1999; 103:2554–2559.

32. Thid D, Holm K, Eriksson PS, Ekeroth J, Kasemo B, Gold J. Journal of Biomedical Materials Research Part A. 2008; 84A:940–953. [PubMed: 17647234]

33. McDonald JC, Duffy DC, Anderson JR, Chiu DT, Wu H, Schueller OJA, Whitesides GM. ELECTROPHORESIS. 2000; 21:27–40. [PubMed: 10634468]

34. Wong I, Ho C-M. Microfluidics and Nanofluidics. 2009; 7:291–306. [PubMed: 20357909]

35. Hillborg H, Gedde UW. Dielectrics and Electrical Insulation, IEEE Transactions on. 1999; 6:703–717.

36. Han Q, Bagheri N, Bradshaw EM, Hafler DA, Lauffenburger DA, Love JC. Proceedings of the National Academy of Sciences. 2012; 109:1607–1612.

37. Varadarajan N, Kwon DS, Law KM, Ogunniyi AO, Anahtar MN, Richter JM, Walker BD, Love JC. Proceedings of the National Academy of Sciences. 2012

38. Song Q, Han Q, Bradshaw EM, Kent SC, Raddassi K, Nilsson Br, Nepom GT, Hafler DA, Love JC. Analytical Chemistry. 2009; 82:473–477. [PubMed: 20000848]

39. Andersson A-S, Glasmästar K, Sutherland D, Lidberg U, Kasemo B. Journal of Biomedical Materials Research Part A. 2003; 64A:622–629. [PubMed: 12601773]

40. Dustin ML. Journal of Structural Biology. 2009; 168:152–160. [PubMed: 19500675]

41. Varadarajan N, Kwon DS, Law KM, Ogunniyi AO, Anahtar MN, Richter JM, Walker BD, Love JC. Proceedings of the National Academy of Sciences. 2012; 109:3885–3890.

42. Picard MD, Cohane KP, Gierahn TM, Higgins DE, Flechtner JB. Vaccine. 2012; 30:4387–4393. [PubMed: 22682294]

43. Gottschalk RA, Hathorn MM, Beuneu H, Corse E, Dustin ML, Altan-Bonnet G, Allison JP. Proceedings of the National Academy of Sciences. 2012; 109:881–886.
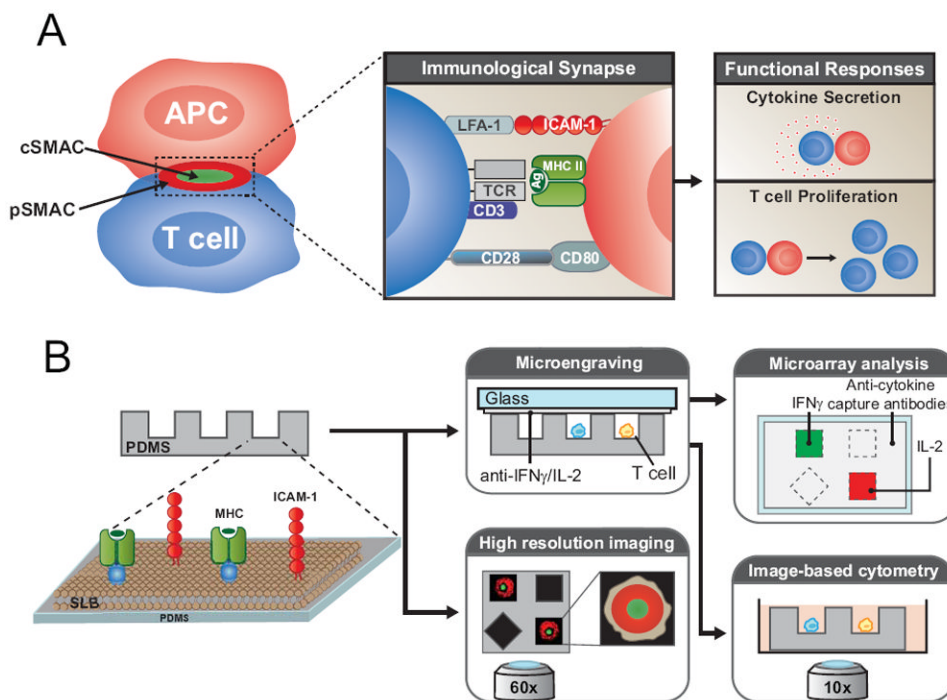
Figure 1. Schematic representation of SLB-tethered ligands in nanowells as APC mimics for T cell activation and single-cell analysis by microengraving

A) Cognate interactions between a T cell and APC initiates a series of receptor-mediated interactions that induce the formation of an immunological synapse and activation of functional responses such as cytokine release and proliferation. B) Arrays of nanowells coated with SLB-anchored ligands (e.g., CD80, MHC class II/peptide and ICAM-1), or antibodies against CD3 and CD28 provide an artificial mimic of an APC, and substrate for measuring both the structure of the synapse by high-resolution imaging and the secretion of cytokines by microengraving. Cell viability and well occupancy can also be assessed by on-chip cytometry.
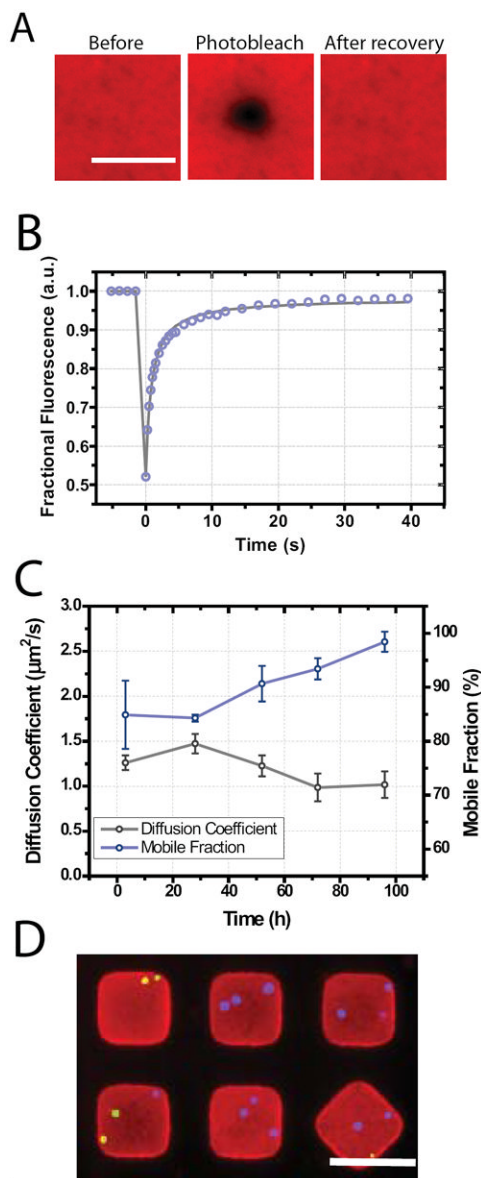
Figure 2. Fluidity and stability of supported lipid bilayers on PDMS
A) Fluorescent images of a region of rhodamine-labeled lipid bilayers before and after local bleaching as well as the subsequent recovery. Scale bar represents 10 µm. B) Representative fluorescence recovery curve from a single region. The circles represent data points and the gray line represents the best fit curve based on the 2D diffusion model. C) Calculated diffusion coefficient and mobile fraction averages (n>5 for each time point) as a function of time at 25°C. Error bars represent standard deviation. D) Composite fluorescence micrograph of T cells cultured for 72h at 37°C on rhodamine-labeled lipid bilayers (red) supported in PDMS nanowells. Viable cells were labeled with Calcein violet (purple) and dead cells with SYTOX green. Scale bar represents 35µm.
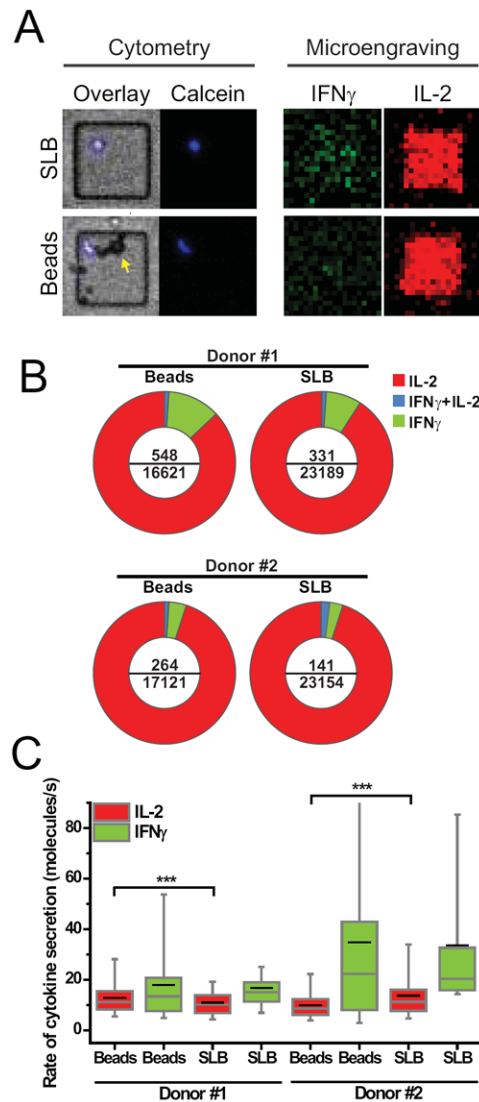
Figure 3. Cytokine secretion from primary T cells stimulated with anti-CD3/CD28 beads or SLBs

A) Representative images of cells labeled with calcein violet inside 50 μm wells and the corresponding printed cytokines (captured on an antibody-coated glass slide by microengraving). The yellow arrow highlights an aggregate of 5μm anti-CD3/CD28 beads in contact with a cell. B) Pie chart of the percentage of single cells secreting IL-2, IFNγ or both from the total secreting population. The numbers inside the charts indicate the total number of secreting cells (top) and the total number of single cells assayed (bottom). C) Quantitative characterization of the rates of cytokine secretion. The box plot shows the rates of secretion for IL-2 and IFNγ were measured for 1 h (after 5 h of stimulation); the plots follow Tukey's convention. The black horizontal lines represent the mean value and the gray horizontal line inside the box represents the median value. Asterisks indicate statistically significant differences between samples (p<0.001) using a two-tailed Mann–Whitney U statistical test.
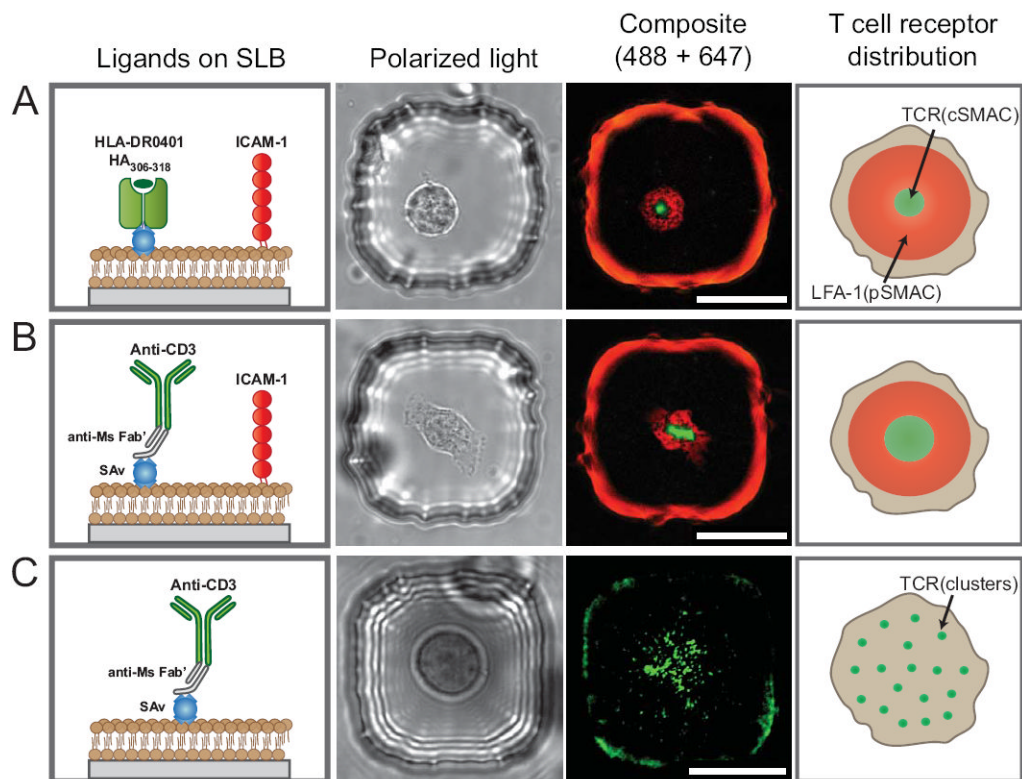
Figure 4. Live-cell imaging of cell activation and formation of the immunological synapse
T cells (HA:D7 clone cell specific for the peptide HA$_{306-318}$) were activated at 37°C with the supported bilayers (inside nanowells of ~30μm diameter) containing (A) pMHC and mouse ICAM-1, (B) anti-CD3 (attached via mono-biotinylated rabbit-anti-mouse Fab' fragment) and mouse ICAM-1, or (C) anti-CD3 only. These representative images were taken 30-40 min after activation by live-cell imaging at 37°C to prevent artifacts from fixation (especially the formation of the pSMAC). Fluorescent background was subtracted to allow for better visualization of the synapse. The visible fluorescence surrounding the wells is due to out-of-focus intensity coming from the Alexa 488-labeled streptavidin or Alexa 647-labeled ICAM-1 attached to the SLB at the side walls. Scale bar represents 20μm.
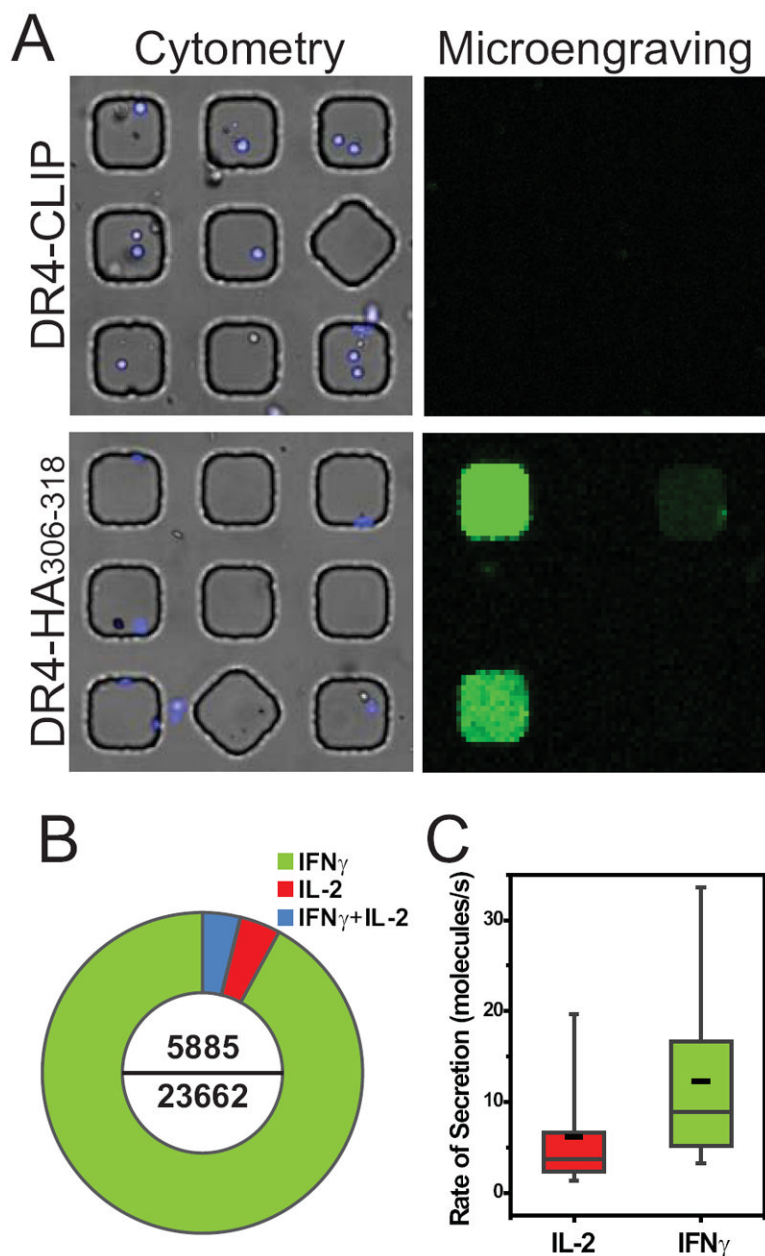
Figure 5. Antigen-specific activation of HA:D7 T cell clone
A) Matched composite images for on-chip cytometry of cells, labeled with calcein violet (blue), inside wells of 50μm diameter and the corresponding microengraving of IFNγ (green; image from scanned microarray). Secreted cytokines were only detected when cells were incubated with HLA-DR*04:01- HA$_{306-318}$ pMHC on the supported lipid bilayer; no cytokine secretion was observed when HLA-DR0401-CLIP (control) was immobilized on the bilayers. Both mono-biotinylated MHC and ICAM-1(His 12) were presented on bilayers containing 0.1 mol% Biotin-Cap-PE, 5 mol% DGS-NTA(Ni) and 94.9 mol% DOPC. B) Pie chart depicting the percentage of single cells secreting IFNγ or IL-2. The numbers inside the donut represent the total number of secreting cells (top) and the total number of single cells assayed (bottom). C) Quantitative analysis of the rates of secretion for IFNγ and IL-2 (molecules/s). The box plot follows Tukey's convention, where the black horizontal lines

represent the mean value and the gray horizontal line inside the box represents the median value.